Multinozzle Emitter Arrays for Nanoelectrospray Mass Spectrometry

Pan Mao[1,4], Hung-Ta Wang[3,4], Peidong Yang[2,3], & Daojing Wang[1,]*

Supporting Information (including Experimental Details and 4 Supplement Figures)

1. EXPERIMENTAL SECTION

1.1. Design and fabrication of MEA chips

All components and their layout on the MEA chips (**Fig. 1a**) were designed using the L-Edit software (v15, Tanner Research Inc., Monrovia, CA). The procedures to fabricate the MEA chips were improved from those for M^3 emitters [1] and involved 9 major steps (**Supplement Fig. 1a-i)**. First, we performed standard photolithography and deep reactive ion etching (DRIE) to pattern and produce channels (with micropillar arrays if needed) and emitters on a 4-inch silicon wafer (**a-c**). Then, we performed second-layer photolithography and DRIE to define and create access holes with a second film mask (**d**). The through-holes provided the opening for oxidant species to reach the sealed channel surface in the following steps. Next, we performed thermal fusion bonding between the patterned wafer and another clean wafer (**e**). The wafers were brought into contact to form spontaneous bonding followed by annealing in the furnace, with N_2 flow at 1050 ºC for 1 hour, to generate covalent fusion bonding. Next, we performed wet oxidation to grow a thick oxide of ~ 1 μm on all silicon surfaces including the sealed channels/emitters (**f**). Afterwards, we performed another photolithography and through-wafer etching steps to sharpen the emitters (left- and right-side, **Fig. 1 and Fig. 2**) and release the chip from the wafer (**g**). The remaining photoresist after etching were removed by oxygen plasma instead of piranha cleaning. Otherwise, piranha solution tended to dissolve photoresist and clog the channels. Subsequently, we sharpened the other two sides (top and bottom, **Fig. 1 and Fig. 2**) of the emitters by mechanically polishing the emitter stem with the sand paper (**h**). Finally, we etched away silicon at the sharpened end of the emitters by selective XeF_2 etching (**i**). This final step ended up with protruding nozzles made of SiO_2. The nozzle length was controlled by tuning the XeF_2 etching cycles. To fabricate freestanding sharpened-end M^3 emitters, we followed the same procedures as described previously for M^3 emitters[1], but introduced an extra polishing step: after the individual emitters were diced from the silicon wafer, they were sharpened on all four edges at one end with the sand paper using a mechanical polishing station, cleaned with a piranha bath, followed by deionized water rinse and N_2 gas blow dry. The fabricated devices were examined by optical microscopy using a Reichert-Jung Polylite 88 microscope (Reichert Microscope Services, Depew, CA), and by scanning electron microscopy (SEM) using a JEOL 6340F FEG-SEM (JEOL Ltd., Tokyo, Japan). Safety considerations: All fabrication procedures were done in the class 100 cleanroom and hence the safety rules and laboratory protocols such as proper handling of toxic chemicals (particularly piranha and HF) must be followed at all times.

The back pressure of the emitters increased with the decrease in nozzle cross sections. This was due to the dramatic increase of hydrodynamic resistance (R), which is roughly inversely proportional to the fourth power of the nozzle diameter (D) (using Hagen-Poiseuille equation for square nozzles: $R \approx 128\mu L/\pi D^4$, μ is viscosity and L is nozzle length); as well as the significant increase of pressure barrier (ΔP) for liquid leakage in microfluidic channels, as estimated by $\Delta P = -2\gamma \cos\theta \cdot (1/h + 1/w)$, where γ and θ are surface tension of the liquid and the contact angle between the liquid and channel walls, respectively, while h and w are channel height and width, respectively[2].

1.2. Electrostatic simulations of MEA emitters

The multiphysics modeling and simulation software COMSOL (v4.1, COMSOL Inc., Burlington, MA) was used to simulate electric fields of MEA emitters with different sharpened features (**Fig. 2**). For simplicity, we did not take into account the presence of complex dynamic gas/fluid behaviors during the actual electrospray process, and only considered static electric fields on MEA emitters relative to the Z-spray sample cone of the Q-TOF API US mass spectrometer (Waters Corp., Milford, MA). Furthermore, we simulated a quadrant instead of the whole device to reduce the dimensions of modeling. Briefly, the static electric field, $E = -\nabla V$, was calculated by solving the classical Poisson's equation $-\nabla \cdot (\varepsilon_0 \varepsilon_r \nabla V) = \rho$, using the 3D electrostatic module, in which ε_0 is the permittivity of free space, ε_r is the relatively permittivity, V is electric scalar potential, and ρ is the space charge density. The simulation involved five major steps: 1. modeling geometry; 2. setting boundary conditions and subdomains; 3. generating mesh; 4. computing solutions; and 5. performing post-processing and visualization. The 3D geometry was constructed with the parameters similar to the actual experimental setup. The dimensions of the sample cone were 5 mm of base radius, 0.5 mm of top radius, and 5 mm of height. The voltage of the stainless steel cone was set at 40 V. The MEA chip had a radius of 40 mm and a thickness of 1 mm. The MEA emitters were equally spaced radially with an angle of 3.75º between adjacent ones. Each emitter consisted of 10 protruding SiO_2 nozzles with inter-nozzle distance of 40 μm. The nozzles had a cross-section of 10 μm × 10 μm and a protruding length of 200 μm. The electric potential of 3 kV was applied to both the Si device and the SiO_2 nozzles, because in real experiments the nozzles were filled with sample solutions and became as conductive as the silicon material. The sample cone and MEA chip were placed in such a way that their central planes (z=0) matched. Zero surface charge was applied to the outer surfaces of the cuboid of 55 mm × 55 mm × 11 mm, which defined the dimension of our modeling. Three types (flat-end, two-side sharpened-end, and four-side sharpened-end) of MEA emitters were simulated to compare the sharpening effects on electric fields of emitter nozzles. The sharpening angles for the left/right side and top/bottom side were 15º and 8º, respectively. Calculated electric fields were analyzed by 3D slice plots on the central plane (z=0). For simplicity, the simulation was done for 1 atm ambient air under the room temperature (25°C).

1.3. Electrospray current measurement of MEA emitters

Total electrospray currents were measured using the Keithley 6487 Picoammeter with built-in data acquisition capabilities (Keithley Instruments, Cleveland, OH). The schematics of the experimental setup is shown in **Supplement Fig. 3** and similar to what was described[3]. Spray tips (Picotips and MEA emitters) were mounted on a translational stage and connected to a dc high-voltage power supply. A stainless steel disk (3cm in diameter) as the counter electrode was positioned and fixed at 2.5 mm from the spray tips with the electrospray axis perpendicular to the disk plane. This disk was directly connected to the picoammeter. A syringe pump (Harvard Apparatus, Holliston, MA) for direct sample infusion was connected to the spray tips through capillary fittings. A solvent mixture of 50:50 methanol/water+1% acetic acid was infused at different flow rates including 0.1, 0.2, 0.4, 0.6, and 1.0 μL/min. The voltage applied to the spray tips ranged from 1.0 kV to 4.8 kV. Each electrospray current under different flow rates and voltages was obtained by averaging 200 consecutive measurements. Standard deviation (s.d.) was calculated for 3-5 individual emitters. Electrospray images were taken using a Waters nanoflow camera kit equipped with a MLH-10× microscope (Computar, Commack, NY), and using a digital camera Nikon 3700 (Nikon Inc., Melville, NY) mounted on a 6×16 monocular (Specwell Corp., Tokyo, Japan). Safety considerations: High voltages supplies should be handled with caution when in use. Solvents containing methanol and acetic acid were handled under the fume hood.

1.4. Nanoelectrospray mass spectrometry

All electrospray MS experiments were performed on a hybrid quadrupole/orthogonal Q-TOF API US mass spectrometer (Waters Corp., Milford, MA). The mass spectrometer was operated in a positive ion mode with a source temperature of 120 ºC and a cone voltage of 40 V. A voltage of 1-5 kV was applied to the MEA emitters or Picotip emitters (i.d. ~10 μm at the tip) (New Objectives Inc., Woburn, MA). The MEA chip was mounted on the voltage stand and manually rotated every 3-4 degrees for each adjacent emitter. TOF analyzer was set in the V-mode. The instrument was calibrated with a multi-point calibration using selected fragment ions from the collision-induced dissociation (CID) of Glu-fibrinopeptide B, GFP B (Sigma, St. Louis, MO). Electrical contact between the voltage stand and MEA chips was made via an aluminum conductive tape. MEA chips were connected with fused silica capillaries (o.d. ~360 μm, i.d. ~100 μm) by polytetrafluoroethylene (PTFE) tubing whose outer diameter (o.d.) matches the i.d. of the access holes (**Fig. 1b**). Torr Seal epoxy (Agilent Technologies, Santa Clara, CA) was applied to permanently seal the connection which could withstand a pressure of more than 100 psi. To test the sensitivity and stability of the emitters, GFP B at a concentration of 0.1 or 1 pmole/μL in a solvent mixture of 50/50 acetonitrile/H_2O+0.1% formic acid was infused directly with a syringe pump at a flow rate of 0.6 μL/min. Data was acquired at 2.4 seconds per scan with 0.1 second between scans. Safety considerations: High voltages applied in the mass spectrometer should be exercised with caution. Solvents containing acetonitrile and formic acid were handled under the fume hood.

1.5. Liquid chromatography-MS/MS

LC-MS/MS analysis was performed using a capillary liquid chromatography system (CapLC) (Waters Corp.) interfaced with a Q-TOF API US mass spectrometer as described [4]. Briefly, 100 fmole of tryptic digests of bovine serum albumin (Michrom Bioresources, Auburn, CA) were injected into the CapLC system through an auto-sampler, pre-concentrated in a 300 μm (i.d.) × 5 mm pre-column packed with PepMap C18 resin (particle diameter of 5 μm and pore size of 100 Å) (Dionex Corp., Sunnyvale, CA), and separated in a 75 μm (i.d.) × 15 cm analytical column packed with the same PepMap C18 resin. The column was equilibrated with solution A containing 3% acetonitrile/97% water/0.1% formic acid, and the peptide separation was achieved with a gradient from 3% to 40% of solution B (95% acetonitrile/5% water/0.1% formic acid) over 32 mins (i.e., from 3 min to 35 min) at a flow rate of ~250 nL/min. This flow rate was achieved by splitting of the 8 μL/min flow from pumps A and B. Peptides eluted from the column were directed through a connecting PTFE Teflon tubing (i.d. ~ 75 μm, o.d. ~ 1.6 mm) to the Picotips or MEA emitters for nanoelectrospray mass spectrometry.

MS/MS spectra were obtained in a data-dependent acquisition (DDA) mode in which the three multiple-charged (+2, +3, +4) peaks with the highest intensity in each MS scan were chosen for CID. Collision energies were set at 10 eV and 30 eV during the MS scan and MS/MS scans, respectively. MS survey scan was 1 second per scan with an inter-scan delay of 0.1 second, while MS/MS scan was 1.9 seconds per scan with an inter-scan delay of 0.1 second. Mass spectra were processed using the MassLynx 4.0 SP4 software. Proteins were identified by Mascot (http://www.matrixscience.com) using the MS/MS peak lists exported from the MassLynx. Protein modifications considered in the search included carboxymethylation of cysteine, N-terminal acetylation, N-terminal Gln to pyroGlu, oxidation of methionine, and phosphorylation of serine, threonine, and tyrosine.

2. SUPPLEMENT FIGURE 1

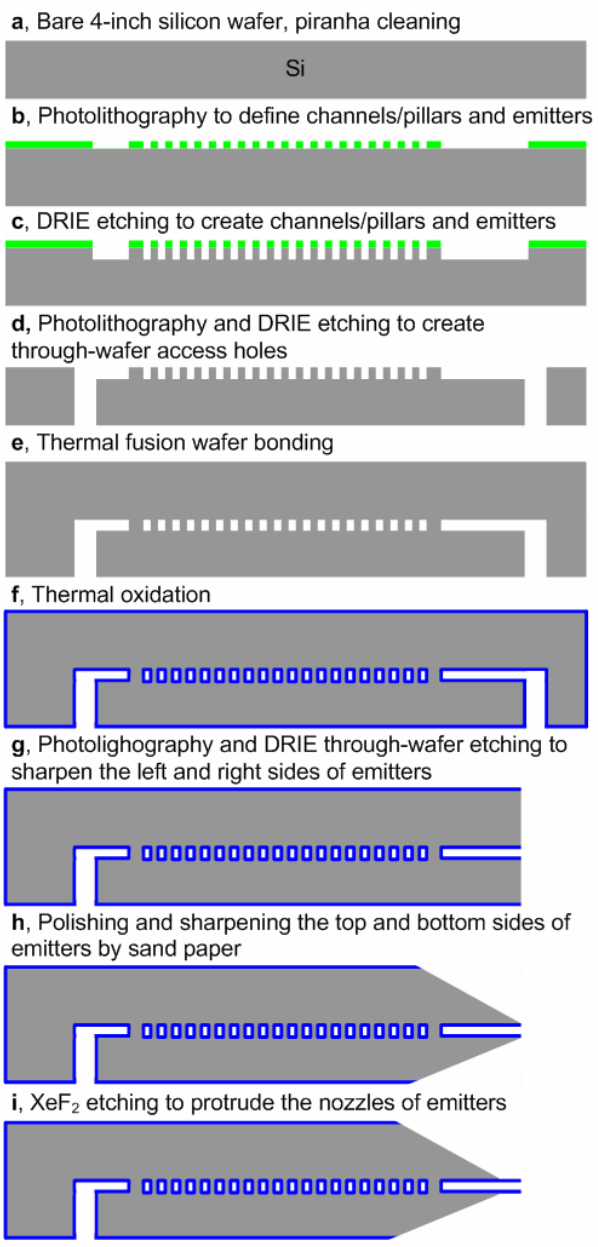

Supplement Figure 1 | Schematics of the fabrication processes for MEA chips. (**a**) Cleaning of 4-inch silicon wafers with a piranha solution. (**b**) Standard photolithography to define fluidic channels, micropillars, and emitters. (**c**) Deep reactive ion etching (DRIE) to create trenches with the desired depth. (**d**) Photolithography, followed by DRIE, to create through-wafer access holes. (**e**) Thermal fusion after cleaning of the wafer, contacting to another clean wafer, and annealing to form covalent Si-Si fusion bonding. (**f**) Growth of thermal oxide on all surfaces. (**g**) Photolithography and through-wafer DRIE to sharpen the left and right sides of emitters and release the MEA chip from the wafer. (**h**) Polishing and sharpening of the top and bottom sides of emitters by the sand paper. (**i**) XeF_2 etching to protrude the nozzles.

3. SUPPLEMENT FIGURE 2

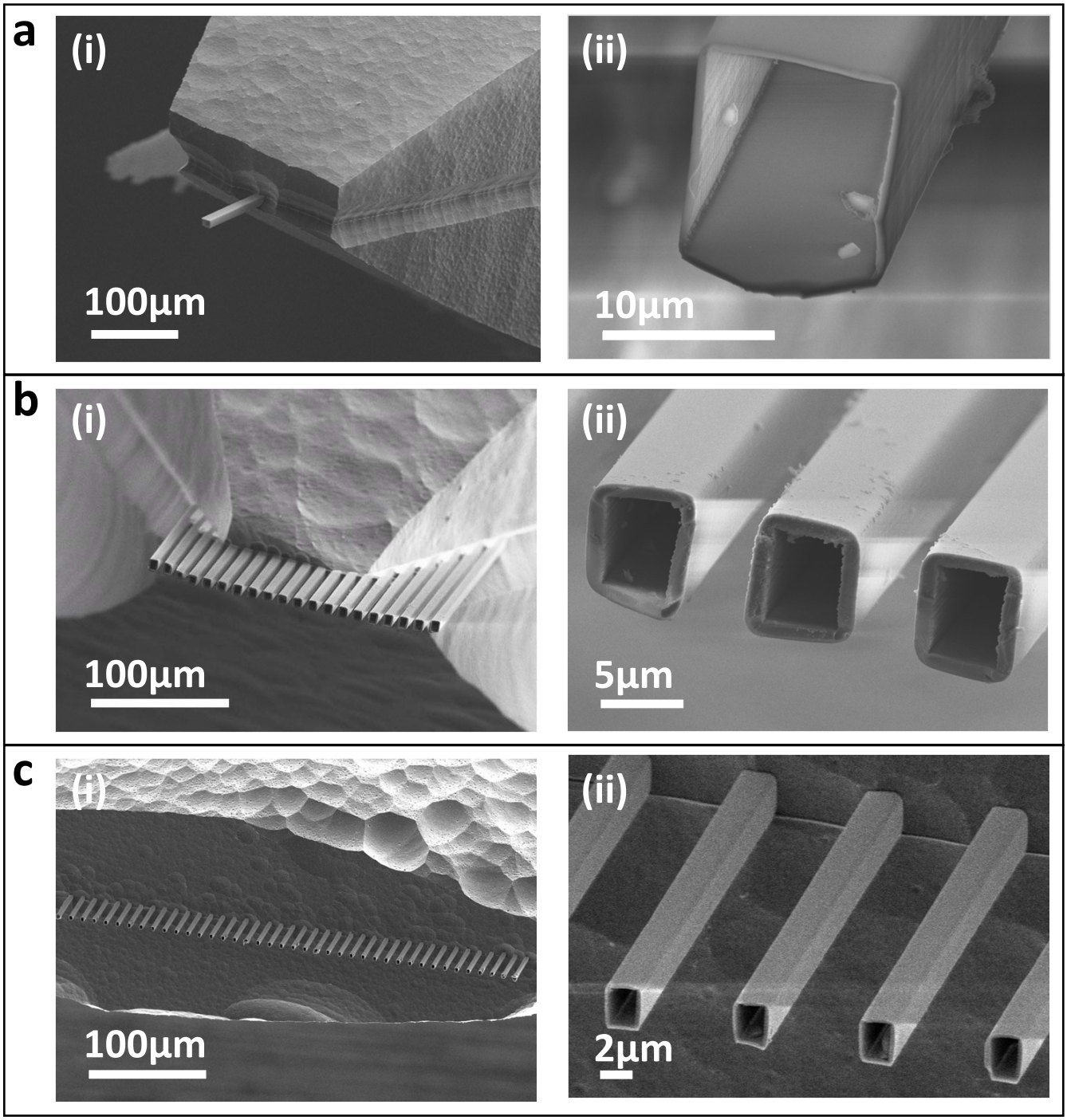

Supplement Figure 2 | SEM images of sharpened-end multinozzle emitters. (**a**) 1-nozzle emitter with a cross-section of 10 µm × 10 µm. (**b**) 20-nozzle emitter with a cross-section of 5 µm × 5 µm. (**c**) 40-nozzle emitter with a cross-section of 2 µm × 2.5 µm. The zoom-out and close-up views of each emitter are shown in the panels (**i**) and (**ii**), respectively.

4. SUPPLEMENT FIGURE 3

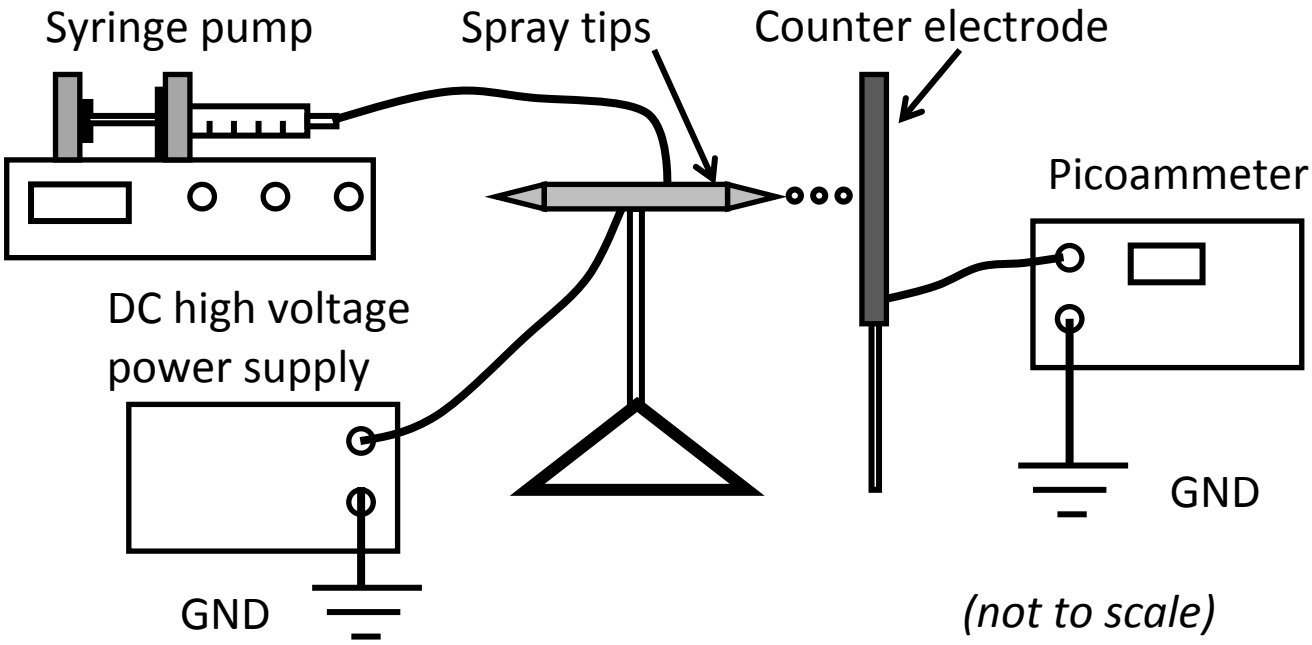

Supplement Figure 3 | Schematics of the experimental setup used for electrospray current measurements. Spray tips were placed on a translational stage with their protruding nozzles perpendicular to a stainless steel disk as the counter electrode. The disk was connected to a picoammeter, which shared the electric ground with the DC high voltage power supply connected to the spray tips. A syringe pump provided direct sample infusion into the spray tips.

5. SUPPLEMENT FIGURE 4

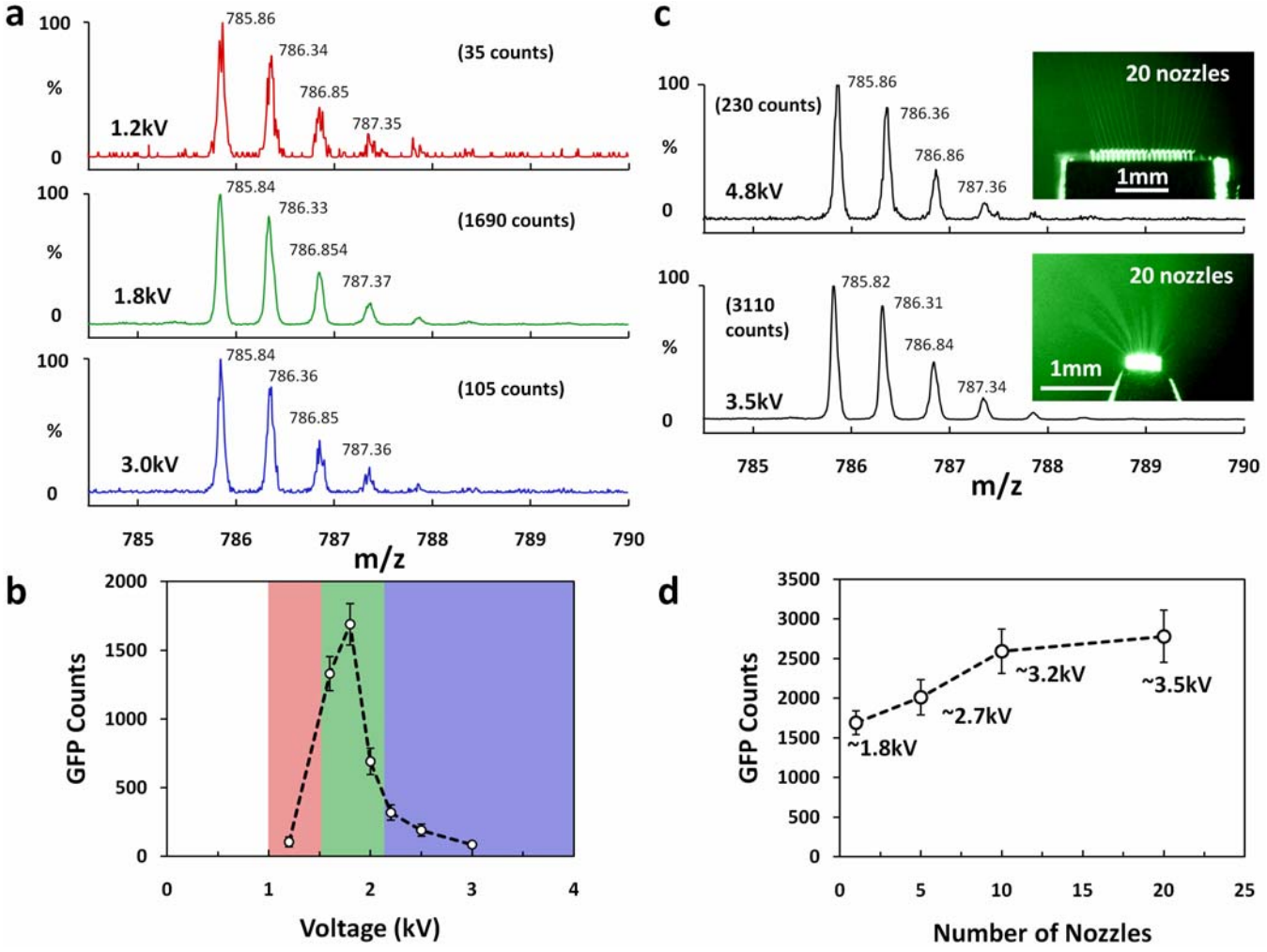

Supplement Figure 4 | Nanoelectrospray mass spectrometry with free-standing multinozzle emitters. (**a**) Voltage dependency of MS sensitivity for sharpened-end single-nozzle M^3 emitters. The mass spectra and GFP counts were obtained for 1 μM GFP B in 50/50 acetonitrile/H_2O+0.1% formic acid with a flow rate of 0.6 μL/min, and under three different voltages of 1.2 kV, 1.8 kV, and 3.0 kV, respectively. (**b**) Corresponding plot showing the dependence of GFP counts on applied voltages. Three different spray modes were observed and classified as pulsating (red), cone-jet (green), and multi-jet modes (blue). (**c**) Comparison of MS sensitivity between a flat-end and a four-side sharpened-end 20-nozzle M^3 emitter. Corresponding optical images of electrospray are shown in the inserts. (**d**) Dependence of MS sensitivity on the number of nozzles for sharpened-end M^3 emitters. The optimal voltages to achieve the stable cone-jet mode spray are designated for each corresponding number of nozzles. All nozzles have a cross-section of 10 μm × 10 μm. Standard deviation (s.d.) was calculated for a 10-minute scan under indicated optimal voltages. Error bar: s.d. (n≥10).

Reference:

(1) Kim, W.; Guo, M.; Yang, P.; Wang, D. *Anal. Chem.* 2007, *79*, 3703-3707.
(2) Hosokawa, K.; Fujii, T.; Endo, I. *Anal. Chem.* 1999, *71*, 4781-4785.
(3) Tang, K.; Lin, Y.; Matson, D. W.; Kim, T.; Smith, R. D. *Anal. Chem.* 2001, *73*, 1658-1663.
(4) Wang, D.; Park, J. S.; Chu, J. S.; Krakowski, A.; Luo, K.; Chen, D. J.; Li, S. *J. Biol. Chem.* 2004, *279*, 43725-43734.